

Supporting Information

Selective Growth of Covalent Organic Framework Ultrathin Films on Hexagonal Boron Nitride

Bing Sun,^{†,‡} Jing Li,^{†,‡} Wei-Long Dong,^{†,‡} Mei-Ling Wu,^{†,‡} Dong Wang^{†,*}

[†] Key Laboratory of Molecular Nanostructure and Nanotechnology and Beijing National Laboratory for Molecular Sciences, Institute of Chemistry, Chinese Academy of Sciences (CAS), Beijing 100190, P. R. China

[‡] University of CAS, Beijing 100049, P. R. China

Correspondence and requests for materials should be addressed to D.W. (email: wangd@iccas.ac.cn, Tel: +86-10-82616953).

S1. Synthesis and characterization of COF-366 powders

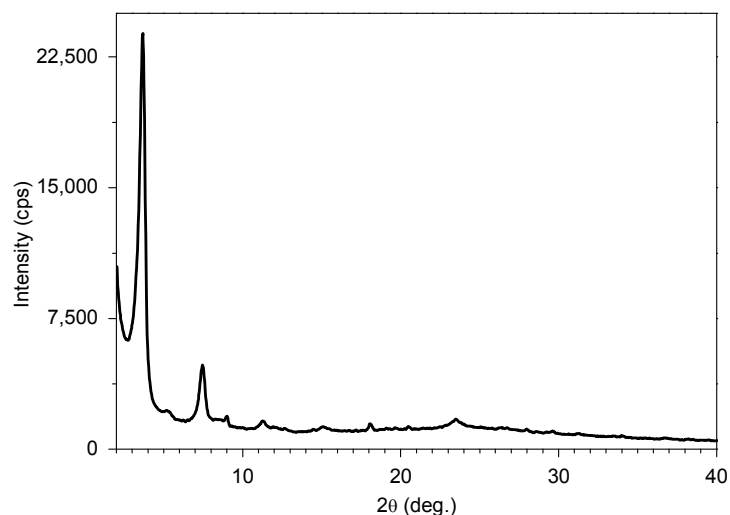


Figure S1 Powder X-ray diffraction (PXRD) pattern of COF-366 powders collected under the mixed solvent of dioxane/methanol in a volume ratio of 3:1 with a higher monomers concentration. COF-366 powders were collected in the similar conditions except for the higher monomers' concentrations: **TAPP** (13.5 mg, 20 μmol), **TPA** (5.6 mg, 40 μmol) in 1,4-dioxane/methanol (v/v 3:1, 1 mL). The PXRD pattern of the collected precipitate was recorded on a PANalytical Empyrean Diffractometer operated at 40 kV and 40 mA with Cu K α radiation ($\lambda = 1.5416 \text{ \AA}$) ranging from 2 to 50° with a speed of 2 °/min at ambient temperature. The PXRD pattern of the crystalline COF-366 powders demonstrates the characteristic diffraction peaks of COF-366 without any impurity diffraction peaks deriving from starting materials, which is in accord with the results in previous work.¹

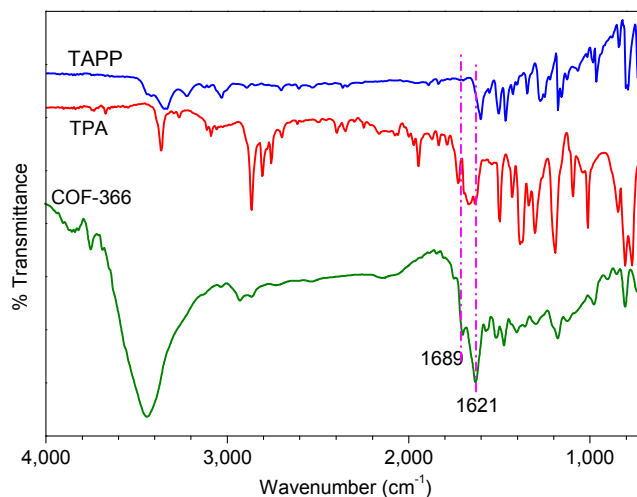


Figure S2 Fourier transform infrared (FTIR) spectra of COF-366 powders and corresponding monomers. The FT-IR spectra were recorded with a Bruker RFS100/S instrument. The emerging FTIR peaks at 1621 and 1249 cm^{-1} reveals the C=N stretching of formed imine functions in COF-366, and FTIR peaks of amino group of **TAPP** at 3440 cm^{-1} and aldehyde group of **TPA** at 1679 cm^{-1} are sharply weakened, indicating the formation of imine between **TAPP** and **TPA**.

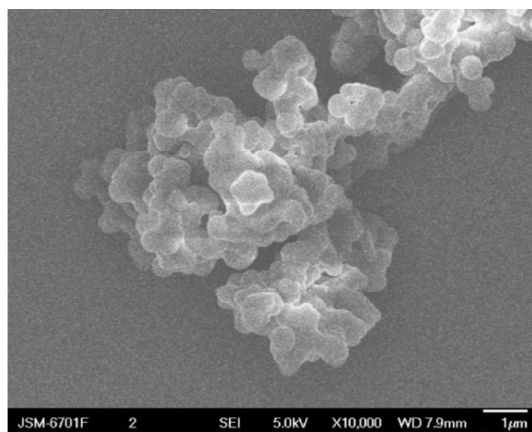


Figure S3 SEM image of COF-366 powders prepared under the solvothermal conditions described in this work, which was recorded on a JEOL JSM-6701F field-emission scanning electron microscope. COF-366 powders show the micro-particle aggregates in this solvothermal conditions.

S2. Electronic structure of TAPP and COF-366 films characterized by XPS

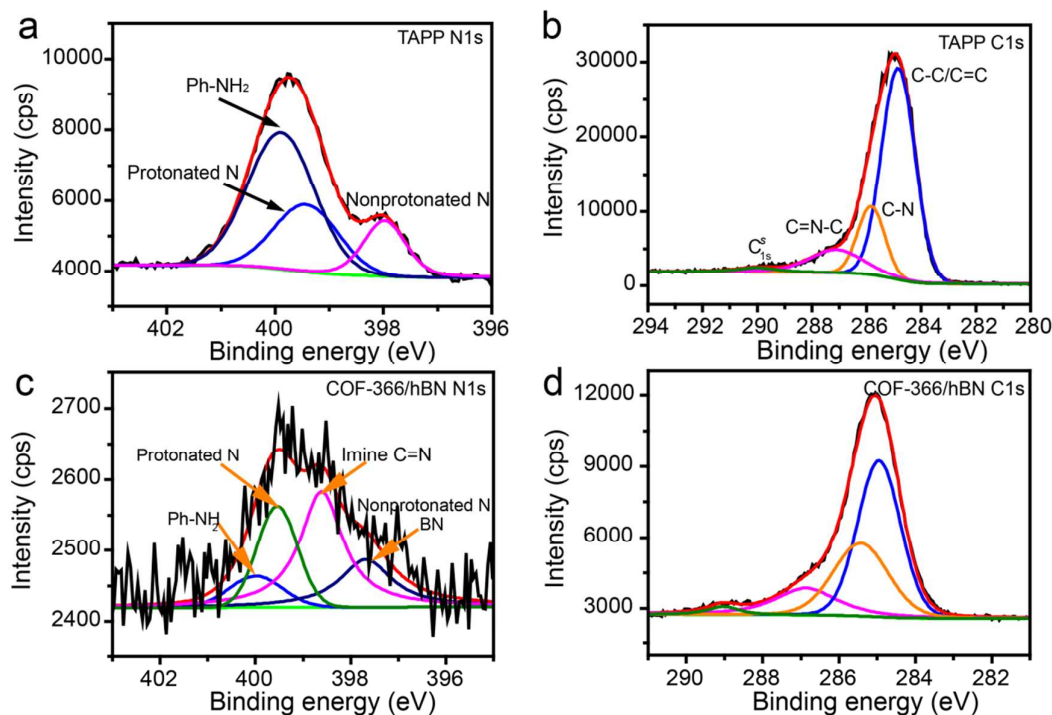


Figure S4 High-resolution XPS spectra of (a) N1s and (b) C1s of **TAPP**, (c) N1s and (d) C1s in COF-366 thin films. The spectrum was smoothed and baseline corrected. X-ray photoelectron spectroscopy (XPS) was performed on the Thermo Scientific ESCALab 250Xi using 200 W monochromated Al K α radiation. The 500 μ m X-ray spot was used for XPS analysis. The base pressure in the analysis chamber was about 3×10^{-10} mbar. Typically the hydrocarbon C1s line at 284.8 eV from adventitious carbon is used for energy referencing.

Table S1 Assignments of XPS peaks of TAPP and COF-366 films referring to previous works.²⁻⁴

| TAPP | | | | COF-366 films | | | |
|--------|--------------------|--------|------------|---------------|--------------------|--------|------------|
| N1s/eV | Assignment | C1s/eV | Assignment | N1s/eV | Assignment | C1s/eV | Assignment |
| 400.2 | Ph-NH ₂ | 284.8 | C-C/C=C | 400.3 | Ph-NH ₂ | 284.9 | C-C/C=C |
| 399.5 | Protonated N | 285.8 | C-N | 399.5 | Protonated | 285.5 | C-N |
| 397.8 | Nonrotonated N | 287.2 | C=N-C | 398.6 | C=N in imine | 286.9 | C=N-C/C=O |
| | | 290.0 | Shake-up | 397.7 | Nonrotonated N/BN | 289.6 | Shake-up |

S3. Selective growth of COF films on hBN with different metal oxide substrate

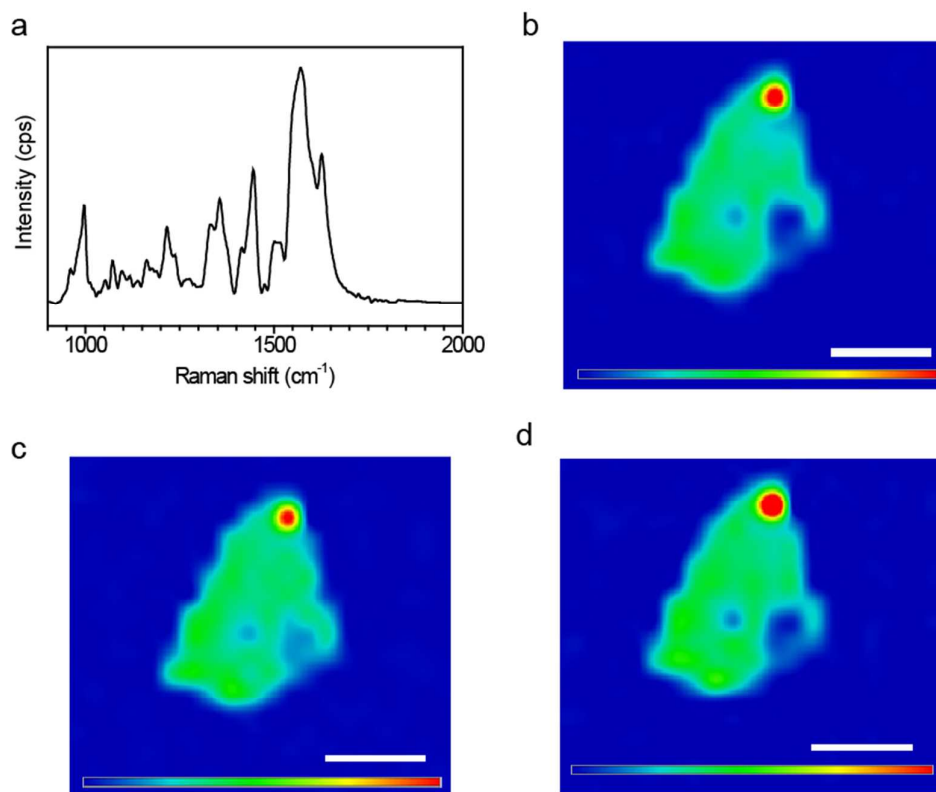


Figure S5 (a) Typical Raman spectra of COF-366 films on hBN/HfO₂/Si (blue), hBN on HfO₂/Si (red) and HfO₂/Si (black) and Raman mapping images of (b) hBN flake at Raman shift of 1363 cm⁻¹ and COF-366 films on hBN/HfO₂/Si surface at Raman shift of (c) 1625 cm⁻¹ and (d) 1570 cm⁻¹. Scale bar: 20 μm; Data scale from 0 to 400 cps.

S4. Absorption spectrum of COF-366 powders

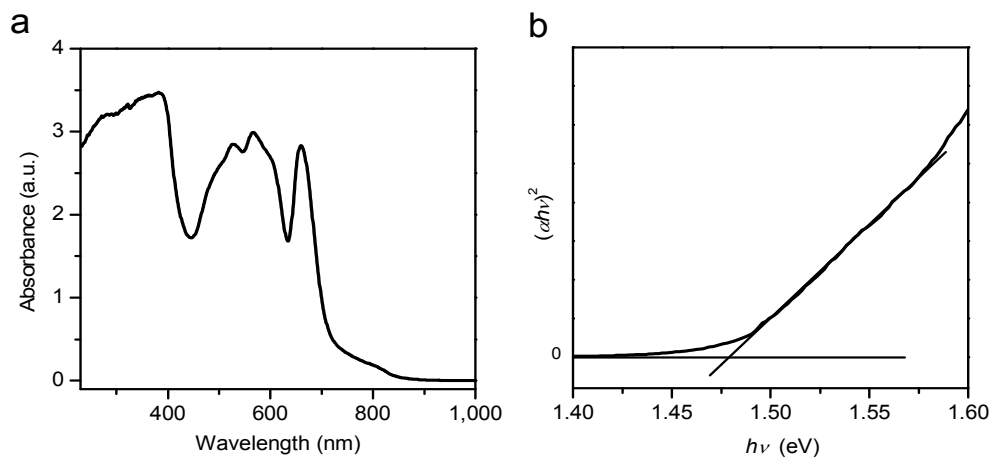


Figure S6 Normalized UV-Vis-NIR absorption spectrum (a) of COF-366 powders growing on hBN surface and the corresponding Tauc's plot (b) for COF-366 powders. The normalized absorption spectra were converted through Kubelka-Munk function from the raw data measured in diffuse reflection mode with an integrating-sphere accessory.

S5. Electronic measurements of COF films/hBN and control experiments

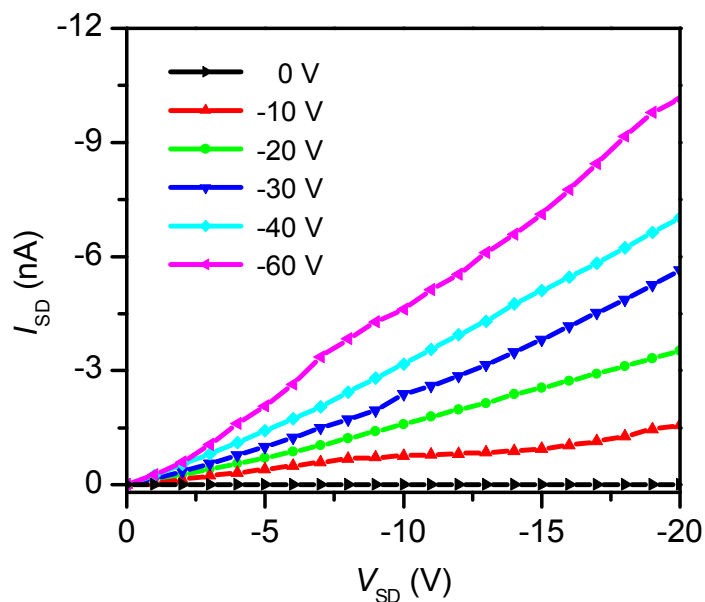


Figure S7 Output characteristics with various bottom-gate voltages for the OFET device fabricated on COF-366 film/hBN/HfO₂/Si(n⁺⁺) wafer.

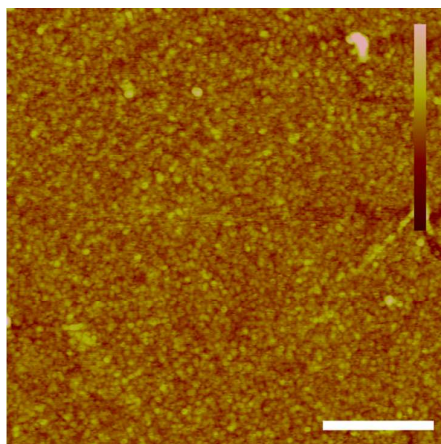


Figure S8 AFM image of COF-366 onto HfO₂ surface by using dioxane as solvent under similar solvothermal conditions. Scale bar: 500 nm, Date scale from 0 to 20 nm. The roughness is evaluated as 1.24 nm.

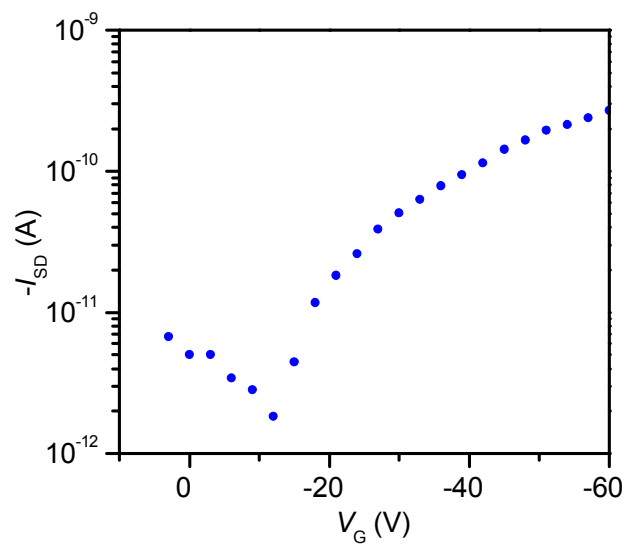


Figure S9 Transfer characteristics for the OFET based on COF-366/HfO₂/Si(n⁺⁺) under the same OFET operating conditions ($V_{SD} = -5$ V).

S6. Grazing incidence X-ray diffraction measurement of COF films on hBN surface

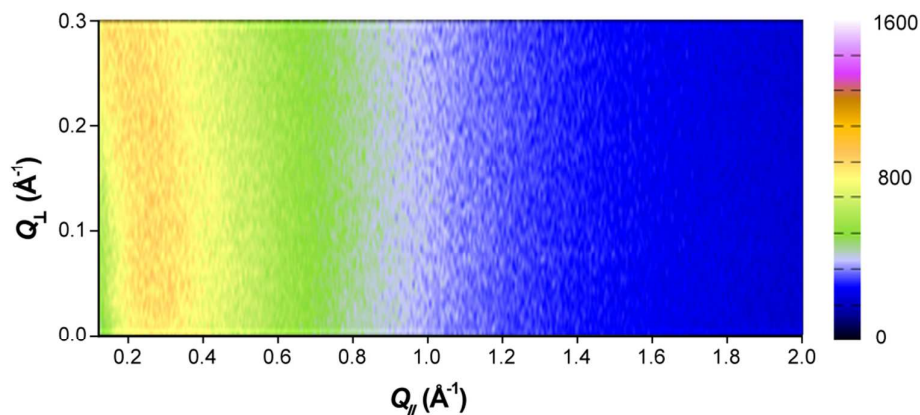


Figure S10. GIXRD data of COF films on hBN surface.

The grazing incidence X-ray diffraction (GIXRD) was performed on a 5-circle Huber diffractometer at the 1W1A station at Beijing Synchrotron Radiation Facility (BSRF) using beam energy of 8.05 keV. The incidence angle α between the beam and sample surface was 0.2° . Axes labels Q_\perp and Q_\parallel are defined using the GISAXS convention $Q_\perp = 4\pi/\lambda \sin(\delta/2)$ and $Q_\parallel = 4\pi/\lambda \sin(\nu/2)$, where δ and ν are the vertical and horizontal scattering angles, respectively. GIXRD is employed to confirm the internal structure of COF films. However, there is no significant diffraction peaks in the case of COF film/hBN as shown in Figure S10.

As reported by W. R. Dichtel's group,⁵ the thinner films grown at 2.2 mM (106 ± 27 nm) “did not exhibit a (100) diffraction peak associated with periodicity in the plane of covalent bonding”. They argued that “it is unclear whether thin films are more disordered in-plane or if all films contain a mixture of amorphous and crystalline domains, such that a higher threshold thickness is needed before

diffraction at small Q_{\perp} is observed.” However, in our present work, the COF films cannot reach to a higher thickness since the thicker films request higher monomer concentrations while higher monomer concentrations can result in the product precipitation in solution rather selectively forming films only on specific substrate. Furthermore, the fact that the size of hBN flakes (tens of micron) is smaller than the diameter of X-ray beam makes it difficult to process GIXRD measurement. Therefore, the thickness and size of selectively grown COF film on hBN restrict the investigation on the crystalline structure of COF films by GIXRD.

References:

- 1 Wan, S.; Gándara, F.; Asano, A.; Furukawa, H.; Saeki, A.; Dey, S. K.; Liao, L.; Ambrogio, M. W.; Botros, Y. Y.; Duan, X.; Seki, S.; Stoddart, J. F.; Yaghi, O. M. Covalent Organic Frameworks with High Charge Carrier Mobility. *Chem. Mater.* **2011**, *23*, 4094-4097.
- 2 Sarno, D. M.; Matienzo, L. J.; Jones, W. E. X-ray Photoelectron Spectroscopy as a Probe of Intermolecular Interactions in Porphyrin Polymer Thin Films. *Inorg. Chem.* **2001**, *40*, 6308-6315.
- 3 Kim, G.; Jang, A. R.; Jeong, H. Y.; Lee, Z.; Kang, D. J.; Shin, H. S. Growth of High-Crystalline, Single-Layer Hexagonal Boron Nitride on Recyclable Platinum Foil. *Nano Lett.* **2013**, *13*, 1834-1839.
- 4 Di Giovannantonio, M.; Kosmala, T.; Bonanni, B.; Serrano, G.; Zema, N.; Turchini, S.; Catone, D.; Wandelt, K.; Pasini, D.; Contini, G.; Goletti, C. Surface-Enhanced Polymerization via Schiff-Base Coupling at the Solid-Water Interface under pH Control. *J. Phys. Chem. C* **2015**, *119*, 19228-19235.
- 5 DeBlase, C. R.; Hernández-Burgos, K.; Silberstein, K. E.; Rodríguez-Calero, G. G.; Bisbey, R. P.; Abruña, H. D.; Dichtel, W. R. Rapid and Efficient Redox Processes within 2D Covalent Organic Framework Thin Films. *ACS Nano* **2015**, *9*, 3178-3183.